Magnetic-Field Control of Photon Echo from the Electron-Trion System in a CdTe Quantum Well: Shuffling Coherence between Optically Accessible and Inaccessible States

L. Langer,[1] S. V. Poltavtsev,[1,2] I. A. Yugova,[1,2] D. R. Yakovlev,[1,3] G. Karczewski,[4] T. Wojtowicz,[4] J. Kossut,[4] I. A. Akimov,[1,3] and M. Bayer[1]

[1]*Experimentelle Physik 2, Technische Universität Dortmund, 44221 Dortmund, Germany*
[2]*Spin Optics Laboratory, St. Petersburg State University, 198504 St. Petersburg, Russia*
[3]*A.F. Ioffe Physical-Technical Institute, Russian Academy of Sciences, 194021 St. Petersburg, Russia*
[4]*Institute of Physics, Polish Academy of Sciences, PL-02668 Warsaw, Poland*

(Received 21 June 2012; published 12 October 2012)

We report on magnetic field-induced oscillations of the photon echo signal from negatively charged excitons in a CdTe/(Cd, Mg)Te semiconductor quantum well. The oscillatory signal is due to Larmor precession of the electron spin about a transverse magnetic field and depends sensitively on the polarization configuration of the exciting and refocusing pulses. The echo amplitude can be fully tuned from the maximum down to zero depending on the time delay between the two pulses and the magnetic-field strength. The results are explained in terms of the optical Bloch equations accounting for the spin level structure of electrons and trions.

DOI: 10.1103/PhysRevLett.109.157403 PACS numbers: 78.67.De, 42.50.Md, 71.35.Ji, 78.47.−p

Coherent optical phenomena in ensembles of atoms or other systems with discrete energy levels have attracted considerable attention in relation to optical quantum memories [1,2]. One important phenomenon in this respect is the photon echo where in a classical picture an intense optical pulse results in rephasing and retrieval of a macroscopic medium's polarization created by a preceding optical pulse. An extension by a third pulse may even stimulate the photon echo such that retrieval occurs on demand [3]. An inherent feature for the emergence of a photon echo is the presence of an inhomogeneity in the system, by which optically imprinted phase information is spread in the ensemble while still being maintained by the individual constituents. Such inhomogeneity is an unavoidable property for many systems of interest. Current experimental activities on quantum light-matter interfaces focus on alkali atoms as well as impurity centers such as rare earth ions or diamond defects [1]. Different protocols using controlled reverse inhomogeneity or atomic frequency combs have been developed in order to overcome noise in conventional photon echo schemes and to increase the optical memory efficiency for single photon applications [2,4,5].

So far, semiconductor nanostructures were not considered as prime candidates mainly due to their high decoherence rates and complex band structures. However, compared to isolated atoms, the fundamental optical excitation in semiconductors, the exciton, possesses a large dipole moment allowing for fast operation. Moreover, its large absorption strength leads to a high efficiency, which is a prerequisite for operation with single photons. On the other hand, there is some tradeoff as a large dipole moment also shortens the exciton lifetime (down to about a nanosecond as compared to possible milliseconds in atomic systems). This is an important obstacle, since the memory should be stored longer than that. For example, after reconversion into a photon, this photon might be interfered with by another photon arriving at a later time. In this respect, charged excitons (trions) open new possibilities in which the associated long-lived electron or hole spin in the ground state can be exploited [6,7]. In quantum dots (QDs) where the spin-orbit interaction is strongly suppressed, the electron spin lifetime may be as long as milliseconds [8]. Significant progress in the coherent optical control of electron spin in charged QDs has been demonstrated by several groups [9–12]. Moreover, spin frequency combs can be prepared using, for example, electron spin mode locking [13]. Thus, an ensemble of trions is prospective for applications in optical memories.

Our concept relies on the photon echo in an electron-trion system subject to transverse magnetic field. The transverse field plays a crucial role here, as it involves electron spins into the echo owing to Larmor precession: the magnetic field introduces a coupling between the spin states along the optical axis that cannot be induced by the optical field. This coupling allows the transfer of coherence superposition in a pair of states that is optically accessible (henceforth termed *bright* coherence) into a superposition in a pair of states that is optically inaccessible (*dark* coherence). In particular, the transfer of the bright coherence into a long-lived, dark electron spin coherence is possible. In what follows, we first describe the main idea of this magnetic-field control, and then present the experimental demonstration for the trions in a semiconductor CdTe/(Cd, Mg)Te quantum well (QW).

The energy and spin level structure of the electron-trion system are schematically shown in Fig. 1. The trion complex comprises two electrons and a hole. In the trion ground state, the electron spins are antiparallel to each other, and therefore the trion is a doublet state based on the total angular momenta of the hole $J = 3/2$. This situation holds not only

 © 2012 American Physical Society

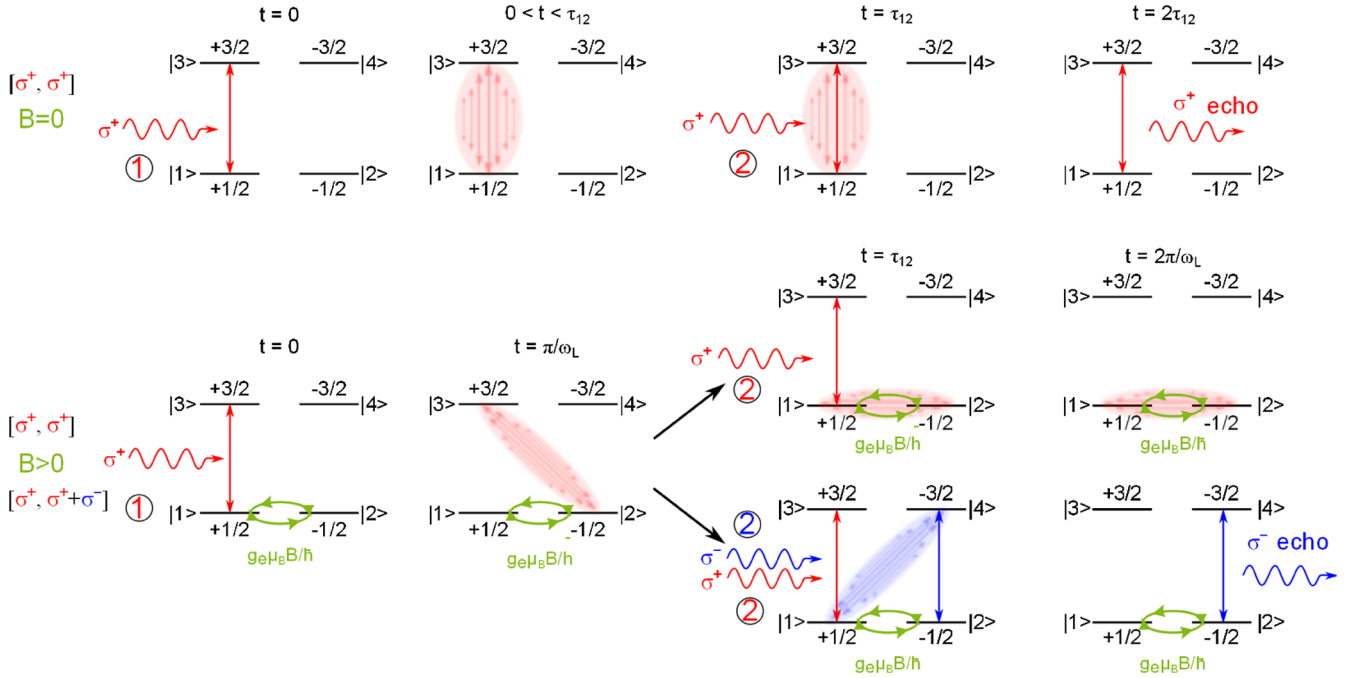

FIG. 1 (color online). Schematic representation of photon echo in the electron-trion system. Time t evolves from left to right. Three different scenarios are considered. The top line shows the photon echo in the two-level system of the $|1\rangle$ and $|3\rangle$ states ($B = 0$, $[\sigma^+, \sigma^+]$). The mid line shows the transfer of optical coherence into electron coherence ($B > 0$, $[\sigma^+, \sigma^+]$), so that no photon echo occurs. The bottom line shows the transfer of optical coherence from the left $|1\rangle - |3\rangle$ two-level system accessible by σ^+-polarized light into the $|2\rangle - |4\rangle$ system addressable by σ^--polarized light. The photon echo is correspondingly σ^- polarized.

for a QW, but also for a QD. Optical excitation couples the electron with possible spin projections $S_z = \pm 1/2$ and the trion doublet with $J_z = \pm 3/2$, respectively, where the quantization z axis is perpendicular to the QW or QD plane. Both doublets are half integer spin states and hence their levels are degenerate in the absence of an external magnetic field. The electric-dipole selection rules allow two optical transitions, $|1\rangle + \sigma^+ \rightarrow |3\rangle$ and $|2\rangle + \sigma^- \rightarrow |4\rangle$, where σ^+ and σ^- denote the respective circular photon polarizations. The system can be considered as a pair of uncoupled oscillators (the left-hand and right-hand columns of the four-level scheme in Fig. 1 are independent). The application of a transverse magnetic field leads to coupling between the electron spin states $|1\rangle$ and $|2\rangle$ and the trion states $|3\rangle$ and $|4\rangle$. For the trions, this effect is small, because the in-plane g factor of the heavy hole is close to zero [14]. Therefore, the main contribution comes from the electron spins with Larmor precession frequency $\omega_L = g_e \mu_B B/\hbar$ around the magnetic field ($\mathbf{B} \parallel x$). Here g_e is the electron g factor and μ_B the Bohr magneton.

We consider a sequence of two optical pulses tuned in resonance with the electron-trion transition and propagating along the z axis (Voigt geometry). Pulse 2, the refocusing pulse, is delayed by time τ_{12} relative to pulse 1 (the excitation pulse). We operate in the short pulse approximation where the pulse duration t_p is significantly shorter than the trion lifetime, the decoherence time, and the electron spin precession period ($\omega_L t_p \ll 1$). Therefore, we can separate the interaction of the electron-trion system with light from its dynamics in magnetic field.

Characteristic scenarios for excitation with a sequence of exciting and refocusing pulses are shown in Fig. 1 for different polarization configurations. For simplicity we neglect decoherence processes here. The top line is at $B = 0$ for σ^+ polarized pulses ($[\sigma^+, \sigma^+]$ configuration). At $t = 0$, optical coherence between the states $|1\rangle$ and $|3\rangle$ is created by the first pulse (solid red arrow). Because of inhomogeneity of the optical transitions, dephasing takes place, so that the macroscopic coherence disappears. This is indicated by the set of arrows of different lengths, symbolizing the phase distribution for the dipoles excited with different frequencies. At $t = \tau_{12}$, pulse 2 conjugates the phase for each dipole, and rephasing starts. At time $t = 2\tau_{12}$, the rephasing has been completed. This results in a photon echo, which is emitted with the same polarization as the two pulses. Note that the photon echo can occur only if both the pulses are copolarized. This scenario would also take place in a two-level system with states $|2\rangle$ and $|4\rangle$ for a sequence of σ^- polarized pulses.

At $B > 0$ the ground state electron precesses (green arrows in Fig. 1). The different coherences showing up now between states $|i\rangle$ and $|j\rangle$ can be associated with nondiagonal elements of the density matrix ρ_{ij}, $i \neq j$. After half of a Larmor precession period, $t = \pi/\omega_L$, the optical coherence ρ_{13} has been fully shuffled to ρ_{23}. The latter represents a "dark" coherence. No photon echo can occur if the system is exposed to a circularly polarized

pulse at this point of time. Nevertheless, the second pulse induces the transition from $|1\rangle$ to $|3\rangle$, which leads to transfer of coherence from ρ_{23} to ρ_{21} (see the second line in Fig. 1). The latter matrix element corresponds to a long-lived electron spin. The microscopic coherence is frozen and stored in the electron spin; i.e., no dephasing or rephrasing will take place, only Larmor precession will occur.

Another interesting scenario takes place when the refocusing pulse is linearly polarized $H = (\sigma^+ + \sigma^-)/\sqrt{2}$, i.e., it contains σ^+ and σ^- polarizations (see the third line of Fig. 1). In this case, ρ_{23} is transferred to ρ_{14}, which is also a dark coherence, but due to Larmor precession, it is finally shuffled into ρ_{24} at $t = 2\tau_{12}$. In addition, rephasing has also been accomplished at this point of time so that a σ^- polarized photon echo is observed.

The complete picture can be developed by solving the Lindblad equation of motion for the (4×4) density matrix $\rho_{ij}(t)$ of the four-level electron-trion system of Fig. 1 [15]. We assume that initially at $t = 0$, the electron spins are unpolarized, i.e., $\rho_{11}(0) = \rho_{22}(0) = 1/2$, while all other elements of the density matrix are zero. In addition, we consider optical pulses of a rectangular temporal profile. The main contributions are summarized in Table I. All other polarization configurations can be constructed from linear combination of these contributions. For example, if we consider a sequence of two linearly copolarized pulses, there is no influence of the magnetic field on the photon echo amplitude. However, if we apply two linearly cross-polarized pulses, the photon echo shows oscillatory behavior. For example, in the $[V, H]$ configuration the photon echo is $V = (\sigma^+ - \sigma^-)/\sqrt{2}$ polarized with an amplitude given by $P_{\mathrm{pe}}^V \propto \cos(\omega_L \tau_{12})$. Obviously P_{pe}^V then changes sign at $\omega_L \tau_{12} = \pi$.

To excite the trion ensemble only, we perform the experiments on a semiconductor QW structure, for which the neutral and charged (trion) excitons are spectrally well separated. The energy level structure of a QW trion is very similar to that in a QD because the trion is typically localized at cryogenic temperatures; only its coherence time is shorter in the QW. The investigated sample comprises five decoupled 20-nm thick CdTe QWs separated by 110 nm $Cd_{0.78}Mg_{0.22}Te$ barriers. Information about the electronic and optical properties, e.g., the electron and hole g factors, spin dephasing, and radiative decay times, can be found in Refs. [14,16].

TABLE I. Nonzero contributions to the photon echo signal for different excitation polarization configurations.

Polarization configuration	Photon echo polarization σ^+	σ^-
$\sigma^+\sigma^+$	$\cos^2(\omega_L\tau_{12}/2)$	0
$\sigma^-\sigma^-$	0	$\cos^2(\omega_L\tau_{12}/2)$
σ^+H	$\frac{1}{2}\cos^2(\omega_L\tau_{12}/2)$	$\frac{1}{2}\sin^2(\omega_L\tau_{12}/2)$
σ^-H	$\frac{1}{2}\sin^2(\omega_L\tau_{12}/2)$	$\frac{1}{2}\cos^2(\omega_L\tau_{12}/2)$

Transient four-wave mixing (FWM) allows direct investigation of coherence in semiconductors (see Ref. [17] and the references therein). So far only a few transient FWM experiments were done on semiconductor structures in a magnetic field [18–22]. Many-body interactions between the distinct magnetoexciton states and their Fano interferences were demonstrated using spectrally broad laser pulses in magnetic fields up to 10 T [19–21]. Here we use spectrally narrow picosecond pulses to excite only, the trion states and minimize many-body interactions. In addition, the experiments are performed at low power densities (pulse energy below 100 $\mathrm{nJ/cm^2}$), corresponding to the linear excitation regime for each pulse. Interferometric heterodyne detection provides high sensitivity for measuring the absolute value of the FWM electric field amplitude in real time t. All measurements were performed at temperature $T = 2$ K. Details about the experimental technique are described in Ref. [23].

The spectral dependence of the FWM signal measured at zero time delay $t = \tau_{12} = 0$ is shown in the inset of Fig. 2(a). There are two peaks corresponding to exciton and trion resonances, labeled X and T, respectively. The PL spectrum coincides well with the FWM signal except for a Stokes shift of about 0.5 meV. This shift indicates spectral diffusion of the exciton and trion complexes to localization sites due to fluctuations of QW width and composition. The trion peak T in the FWM spectrum is located at 1.5997 eV, and is red shifted relative to the exciton X by the binding energy of 2.2 meV. A time-resolved FWM amplitude measured at the T resonance is shown in Fig. 2(a). At time delays $\tau_{12} < 10$ ps the form of the signal contains signatures for free polarization decay. At later delays, the coherent response is given by a Gaussian-like pulse, appearing at a delay time of $t = 2\tau_{12}$, thereby representing a photon echo from an inhomogeneously broadened ensemble of trions. Therefore, the FWM signal measured at $t = 2\tau_{12}$, which is shown by the solid line in Fig. 2(a), directly reflects the photon echo amplitude $|P_{\mathrm{pe}}|$ for time delays $\tau_{12} > 10$ ps. It decays exponentially with increasing τ_{12} and can be well described by $|P_{\mathrm{pe}}| \propto \exp(-2\tau_{12}/T_2)$ (see the dashed line in Fig. 2(a)). The coherence time $T_2 = 25$ ps obtained from the fit agrees well with previous studies of similar p-doped QWs [24].

The decays $|P_{\mathrm{pe}}(\tau_{12})|$ for different polarization configurations are summarized in Fig. 2(b). The configurations are denoted by ABC, where A and B are the polarizations of the excitation and refocusing pulses 1 and 2, respectively, and C is the polarization of the resulting photon echo amplitude. For zero magnetic field, the temporal behavior of the signal is shown for the HHH, HVH, and $\sigma^+\sigma^+\sigma^+$ configurations. Here both the coherence times and the amplitudes are nearly the same, indicating that many-body interactions can be neglected [17]. At $B = 0.7$ T strong oscillations occur for the HVH and $\sigma^+\sigma^+\sigma^+$ configurations [see Fig. 2(c)]. These oscillations appear also when the magnetic field B is scanned.

For convenience we consider the ratio $R = |P_{\mathrm{pe}}(\tau_{12}, B)|/|P_{\mathrm{pe}}(\tau_{12}, B = 0)|$ to isolate the oscillatory

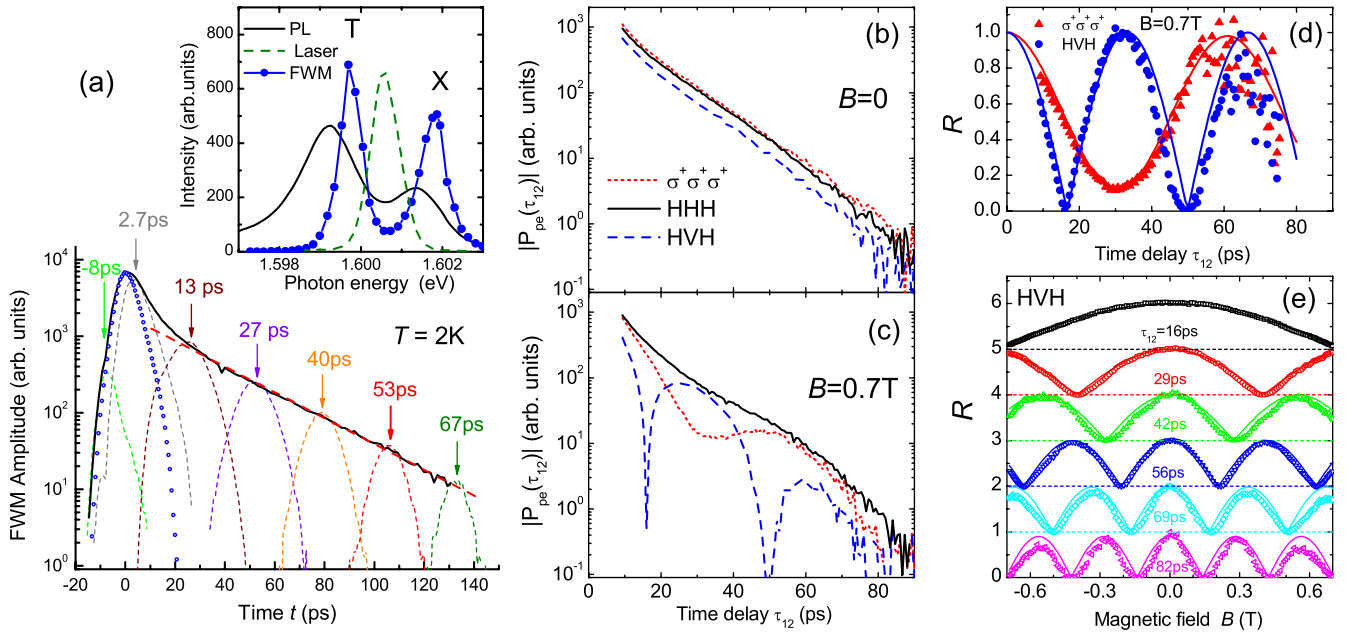

FIG. 2 (color online). (a) Demonstration of photon echo. The dashed curves correspond to time-resolved four-wave mixing amplitudes measured for different time delays τ_{12}, as indicated also at the arrows. Open symbols as well as the solid line give the FWM signal decay at $t = \tau_{12}$ and $t = 2\tau_{12}$, respectively; $t = 0$ corresponds to pulse 1 arrival time. The dashed line is fit by exponential decay. Inset: spectra of FWM signal measured at $t = \tau_{12} = 0$, PL, and typical spectral shape of the laser line. PL spectrum is measured for cw excitation with photon energy 2.33 eV. (b) and (c) Photon echo amplitude as function of τ_{12} for three different excitation-detection polarization configurations HHH, HVH, and $\sigma^+\sigma^+\sigma^+$ at $B = 0$ (b) and $B = 0.7$ T (c). (d) Ratio R as defined in text as function of τ_{12} in the HVH (circles) and $\sigma^+\sigma^+\sigma^+$ (triangles) configurations. (e) Magnetic-field dependence of R in HVH configuration. The solid lines in (d) and (e) are theory curves according to Table I. The oscillation frequency Ω is determined by $|g_e| = 1.67$ in $\sigma^+\sigma^+\sigma^+$ and $|g_e - g_{h,\perp}| = 1.54$ in HVH configuration.

part, assuming that T_2 is not altered for magnetic fields up to $B = 1$ T. The temporal and magnetic-field dependencies of $R(\tau_{12}, B)$ are presented in Figs. 2(d) and 2(e). In full agreement with our expectations (see Table I), R follows a $\cos^2(\Omega\tau_{12}/2)$ dependence in the $\sigma^+\sigma^+\sigma^+$ configuration, while for the HVH configuration R oscillates as $|\cos(\Omega\tau_{12})|$. For the $\sigma^+\sigma^+\sigma^+$ configuration we take into account the constant background $R_0 = 0.12$ resulting from residual linear polarization of the laser pulses. For cocircularly polarized pulses, the oscillation frequency Ω corresponds to the electron Larmor precession frequency ω_L given by $|g_e| = 1.67$, while in the HVH configuration we evaluate a somewhat smaller frequency. Here Larmor precession of the heavy hole in the trion state contributes to the photon echo oscillations resulting in $\Omega = |g_e - g_{h,\perp}|\mu_B B/\hbar$, where $g_{h,\perp}$ is the transverse heavy hole g factor [15]. From the experimental data we find $|g_{h,\perp}| = 0.13$, which is in agreement with previous studies of the same sample [14].

In conclusion we have demonstrated the magnetic control of photon echo from the electron-trion system of a semiconductor QW. Exploiting the Larmor precession of electron spins in a transverse magnetic field, we demonstrate the transfer of coherence between optically accessible and inaccessible state superpositions. This allows us to suppress the photon echo amplitude or change its sign depending on the magnetic-field strength and delay between the exciting and refocusing pulses. The observed signals can be well described by the optical Bloch equations taking into account the spin level structure of electron and trion. Singly charged QDs with strong confinement and long coherence times have large potential for shuffling the coherences between the electronic spin states. Note that the external magnetic field can be substituted by effective magnetic fields produced by the nuclei or magnetic impurities due to hyperfine or exchange interactions.

This work was supported by the Deutsche Forschungsgemeinschaft (Grant No. AK-40/3 and priority program SPP1285 AK-40/4) and BMBF project QuaHL-Rep. Research in Poland was partially supported by the European Union within the European Regional Development Fund, through Innovative Economy Grant No. POIG.01.01.02-00-008/08. I.A.Y. is a Fellow of the Alexander von Humboldt Foundation. The authors are grateful to V. L. Korenev, I. Ya. Gerlovin, and J. Debus for useful discussions.

[1] K. Hammerer, A. S. Sørensen, and E. S. Polzik, Rev. Mod. Phys. **82**, 1041 (2010).
[2] A. I. Lvovsky, B. C. Sanders, and W. Tittel, Nature Photon. **3**, 706 (2009).

[3] S. Mukamel, *Principles of Nonlinear Spectroscopy* (Oxford University, New York, 1995).
[4] M. Afzelius, I. Usmani, A. Amari, B. Lauritzen, A. Walther, C. Simon, N. Sangouard, J. Minář, H. de Riedmatten, N. Gisin, and S. Kröll, Phys. Rev. Lett. **104**, 040503 (2010).
[5] E. Saglamyurek, N. Sinclair, J. Jin, J. A. Slater, D. Oblak, F. Bussiéres, M. George, R. Ricken, W. Sohler, and W. Tittel, Nature (London) **469**, 512 (2011).
[6] *Semiconductor Qubits*, edited by F. Henneberger and O. Benson (Pan Stanford Publishing, Singapore, 2008).
[7] *Spin Physics in Semiconductors*, edited by M. Dyakonov (Springer-Verlag, Berlin, 2008).
[8] M. Kroutvar, Y. Ducommun, D. Heiss, M. Bichler, D. Schuh, G. Abstreiter, and J. J. Finley, Nature (London) **432**, 81 (2004).
[9] D. Press, T. D. Ladd, B. Zhang, and Y. Yamamoto, Nature (London) **456**, 218 (2008).
[10] J. Berezovsky, M. H. Mikkelsen, N. G. Stoltz, L. A. Coldren, and D. D. Awschalom, Science **320**, 349 (2008).
[11] X. Xu, B. Sun, P. R. Berman, D. G. Steel, A. S. Bracker, D. Gammon, and L. J. Sham, Nature Phys. **4**, 692 (2008).
[12] A. Greilich, S. E. Economou, S. Spatzek, D. R. Yakovlev, D. Reuter, A. D. Wieck, T. L. Reinecke, and M. Bayer, Nature Phys. **5**, 262 (2009).
[13] A. Greilich, D. R. Yakovlev, A. Shabaev, A. L. Efros, I. A. Yugova, R. Oulton, V. Stavarache, D. Reuter, A. Wieck, and M. Bayer, Science **313**, 341 (2006).
[14] E. A. Zhukov, D. R. Yakovlev, M. Bayer, M. M. Glazov, E. L. Ivchenko, G. Karczewski, T. Wojtowicz, and J. Kossut, Phys. Rev. B **76**, 205310 (2007).
[15] See Supplemental Material at http://link.aps.org/supplemental/10.1103/PhysRevLett.109.157403 for derivation of the photon echo amplitude in different polarization configurations.
[16] G. Bartsch, M. Gerbracht, D. R. Yakovlev, J. H. Blokland, P. C. M. Christianen, E. A. Zhukov, A. B. Dzyubenko, G. Karczewski, T. Wojtowicz, J. Kossut, J. C. Maan, and M. Bayer, Phys. Rev. B **83**, 235317 (2011).
[17] D. S. Chemla and J. Shah, Nature (London) **411**, 549 (2001).
[18] O. Carmel and I. Bar-Joseph, Phys. Rev. B **47**, 7606 (1993).
[19] U. Siegner, M.-A. Mycek, S. Glutsch, and D. S. Chemla, Phys. Rev. Lett. **74**, 470 (1995).
[20] S. T. Cundiff, M. Koch, W. H. Knox, J. Shah, and W. Stolz, Phys. Rev. Lett. **77**, 1107 (1996).
[21] P. Kner, W. Schäfer, R. Lövenich, and D. S. Chemla, Phys. Rev. Lett. **81**, 5386 (1998).
[22] J. A. Davis, J. J. Wathen, V. Blanchet, and R. T. Phillips, Phys. Rev. B **75**, 035317 (2007).
[23] See Supplemental Material at http://link.aps.org/supplemental/10.1103/PhysRevLett.109.157403 for description of the experimental technique.
[24] D. Brinkmann, J. Kudrna, P. Gilliot, B. Hönerlage, A. Arnoult, J. Cibert, and S. Tatarenko, Phys. Rev. B **60**, 4474 (1999).